Institute of Electronics, Information, and Communication Engineers

IEICE TRANS. COMMUN., VOL.E90–B, NO.4 APRIL 2007

PAPER

Optimal Antenna Matching and Mutual Coupling Effect of Antenna Array in MIMO Receiver

Hiroki IURA[†a)], *Student Member*, **Hiroyoshi YAMADA**[††b)], **Yasutaka OGAWA**[†††], *and* **Yoshio YAMAGUCHI**[††], *Members*

SUMMARY Antenna array is essential factor for multiple- input multiple-output (MIMO) wireless systems. Since the antenna array is composed of closely spaced elements, the mutual coupling among the elements cannot be ignored for the best performance of the array. Mutual coupling affects the MIMO channel, so the performance of a MIMO system, including channel capacity and diversity, varies with the degree of mutual coupling. The effect of mutual coupling is a function of the antenna load impedance. Therefore, designing an optimal element-matched array for a MIMO system requires consideration of the optimal matching condition for the array elements, the one that maximizes the channel capacity. We evaluated the effects of mutual coupling with various matching conditions in dipole arrays, and investigated their effects on the path correlation and channel capacity of MIMO systems. Simulation showed that the conventional conjugate matching of each element is still suitable for closely spaced elements except when the separation is about less than 0.1λ. Theoretical consideration of the received power of a closely-spaced-element array is also provided to show the effects of mutual coupling.

key words: *MIMO, mutual coupling, antenna matching, channel capacity, correlation*

1. Introduction

There is a growing demand for high-rate transmission systems, particularly for mobile subscriber units to support multimedia mobile communications. One approach to meet this demand is the use of a Multiple-Input Multiple-Output (MIMO) wireless system with multiple elements at both the transmitter and receiver. The MIMO system increases transmission capacity by transmitting simultaneous as well as independent streams in a rich heavy multipath environment [1].

The use of antenna array often affects system performance due to mutual coupling among the elements. While using wide element spacing can prevent this coupling, this is not a realistic approach for some systems. For example, close element spacing is needed in mobile terminals due to size requirements. Close antenna element spacing often causes severe mutual coupling and highly correlated fading. These effects must be taken into account when considering MIMO channel transfer matrix. Since the performance of a MIMO system depends on the channel matrix, an analysis of the mutual coupling and the element spacing is very important [2]. Wallace and Jensen examined the characteristics of a MIMO system with dipole arrays with various spacings [3]. They inserted a matching network to maximize the received power between the antennas and the receiver (terminated loads), and analyzed the optimization problem using network theory based on the scattering parameter (S-parameter). This approach is closely related to optimize a receiving array by inserting a decoupling network [4]. While such multiport optimization approaches maximize MIMO channel capacity, it is sometimes difficult to design an optimal network.

In this paper, we consider a simple optimization approach. We consider only the antenna matching condition between the array elements and receiver (terminated loads). Although this approach produces a sub-optimal solution, it nevertheless illustrates how MIMO channel capacity can be improved by simply adjusting the matching condition of the elements. Furthermore, it also clarifies the effects of the mutual coupling and antenna matching at the receiver. The antenna matching condition is a key design factor, so clarifying the optimal antenna matching condition should be quite useful to antenna engineers.

In this paper, we analyze the channel capacity of a MIMO receiver with a dipole array with various element spacings. Three types of antenna matching conditions are considered: 1) conjugate matching to the self-impedance of each element (Z_{11}^*), 2) conjugate matching to the input/port impedance (Z_{in}^*), and 3) optimal antenna matching that maximizes channel capacity. The element patterns and eigenpath gains are also shown as well as the received power and their path correlation. In addition, theoretical results for the effect of mutual coupling on received power are provided for arrays having elements with very close spacing. These results help clarify the effects of mutual coupling on MIMO capacity.

The paper is organized as follows. In Sect. 2, we formulate the channel capacity problem, including the mutual coupling effect under the antenna matching condition. Section 3 describes the simulation, which uses two-element dipole arrays and the method of moments, and presents some of the results, including the channel capacity, path correlation, and so forth as a function of element spacing in a Rayleigh fading environment. In Sect. 4, we discuss theoret-

Manuscript received November 29, 2005.
Manuscript revised March 24, 2006.

[†]The author is with Graduate School of Science & Technology, Niigata University, Niigata-shi, 950-2181 Japan.
[††]The authors are with Faculty of Engineering, Niigata University, Niigata-shi, 950-2181 Japan.
[†††]The author is with Graduate School of Information Science & Technology, Hokkaido University, Sapporo-shi, 060-8628 Japan.
a) E-mail: hiroki@wave.ie.niigata-u.ac.jp
b) E-mail: yamada@ie.niigata-u.ac.jp

DOI: 10.1093/ietcom/e90–b.4.960

Copyright © 2007 The Institute of Electronics, Information and Communication Engineers

NII-Electronic Library Service

Institute of Electronics, Information, and Communication Engineers

ically the effect of mutual coupling on the received power of closely spaced two-element dipole arrays. Results and some remarks are summarized in Sect. 5.

2. Formulation of the Problem

2.1 SVD-MIMO

The MIMO transmission model embedded an M-element transmitting array and an N-element receiving array ($M \times N$ MIMO) is depicted in Fig. 1. The channel transfer matrix $\boldsymbol{H}$ in this model is represented by

$$\boldsymbol{H} = \begin{bmatrix} h_{11} & h_{12} & \cdots & h_{1M} \\ h_{21} & h_{22} & \cdots & h_{2M} \\ \vdots & \vdots & \ddots & \vdots \\ h_{N1} & h_{N2} & \cdots & h_{NM} \end{bmatrix}, \tag{1}$$

where h_{ij} is the channel response from the j-th transmitting signal to the i-th receiving signal. By applying singular value decomposition (SVD) to $\boldsymbol{H}$, we can write (1) as

$$\boldsymbol{H} \equiv \boldsymbol{E}_r \boldsymbol{D} \boldsymbol{E}_t^H, \tag{2}$$

$$\boldsymbol{D} \equiv \begin{bmatrix} \sqrt{\lambda_1} & 0 & 0 & 0 \\ 0 & \sqrt{\lambda_2} & 0 & 0 \\ 0 & 0 & \ddots & 0 \\ 0 & 0 & 0 & \sqrt{\lambda_{m_0}} \end{bmatrix}, \tag{3}$$

$$\boldsymbol{E}_t \equiv [\boldsymbol{e}_{t,1} \quad \boldsymbol{e}_{t,2} \quad \cdots \quad \boldsymbol{e}_{t,m_0}], \tag{4}$$

$$\boldsymbol{E}_r \equiv [\boldsymbol{e}_{r,1} \quad \boldsymbol{e}_{r,2} \quad \cdots \quad \boldsymbol{e}_{r,m_0}], \tag{5}$$

$$m_0 = \min(M, N), \tag{6}$$

where ^{H} denotes the Hermitian or complex conjugate transpose and λ_i is the i-th eigenvalue of $\boldsymbol{H}\boldsymbol{H}^H$ or $\boldsymbol{H}^H\boldsymbol{H}$. The $\boldsymbol{e}_{t,i}$ is the eigenvector corresponding to the λ_i of $\boldsymbol{H}^H\boldsymbol{H}$, and $\boldsymbol{e}_{r,i}$ is the eigenvector corresponding to the λ_i of $\boldsymbol{H}\boldsymbol{H}^H$. These formulations show that m_0 independent transmission paths can be formed using weight vectors corresponding to the eigenvectors. These weight vectors enable the signals to be decoded correctly at the receiver.

$$\boldsymbol{E}_r^H \boldsymbol{v} = \mathrm{diag}[\sqrt{\lambda_1} \quad \sqrt{\lambda_2} \quad \cdots \quad \sqrt{\lambda_{m_0}}]\boldsymbol{s}, \tag{7}$$

where $\boldsymbol{v}$ is an $N \times 1$ receiving vector and $\boldsymbol{s}$ is an $m_0 \times 1$ transmission vector. Each independent transmission path is called an eigen-path, and its amplitude gain $\sqrt{\lambda_i}$ is proportional to the amplitude of the signal flowing along the path.

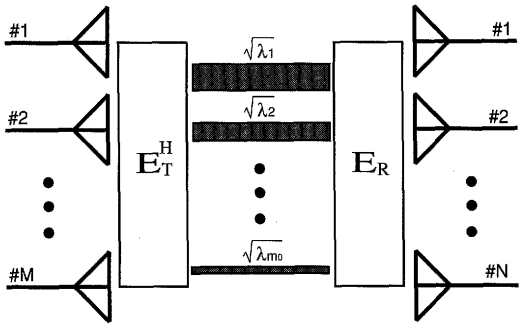

Fig. 1 MIMO transmission path model.

2.2 Channel Matrix

When the array has widely spaced elements, the channel matrix depends mostly on the propagation environment. When the array has closely spaced elements, the channel matrix is also affected by both the mutual coupling and the spatial correlation. To simplify this analysis, we assume that the transmitting array is ideal (no mutual coupling or infinite element spacing ($d \to \infty$)). Although we focus on the receiving array optimization problem to clarify the effect of mutual coupling on the array, the following formulations are also applicable to the transmitting array. The channel matrix combining the effects of the propagation environment and the mutual coupling is given by

$$\tilde{\boldsymbol{H}} = \boldsymbol{C}\boldsymbol{H}_s, \tag{8}$$

where $\boldsymbol{C}$ is the mutual coupling matrix and $\boldsymbol{H}_s$ is the channel matrix determined by the propagation environment. The mutual coupling matrix can be defined by the self/mutual impedance of the array [5], [6].

$$\boldsymbol{C}^{-1} = \begin{bmatrix} 1 + \frac{Z_{11}}{Z_{L1}} & \frac{Z_{12}}{Z_{L2}} & \cdots & \frac{Z_{1N}}{Z_{LN}} \\ \frac{Z_{21}}{Z_{L1}} & 1 + \frac{Z_{22}}{Z_{L2}} & \cdots & \frac{Z_{2N}}{Z_{LN}} \\ \vdots & \vdots & \ddots & \vdots \\ \frac{Z_{N1}}{Z_{L1}} & \frac{Z_{N2}}{Z_{L2}} & \cdots & 1 + \frac{Z_{NN}}{Z_{LN}} \end{bmatrix}, \tag{9}$$

where Z_{Li} is the load impedance of the i-th element.

2.3 Complex Power Correlation Matrix

To evaluate the mutual coupling effect, it is necessary to evaluate the eigen-path power as a function of both the terminal voltage and the load impedance of the elements. We thus introduce the following complex power correlation matrix for deriving the eigen-path power.

$$\begin{aligned} \boldsymbol{R}_p &= \frac{1}{2}\mathrm{E}\left[\boldsymbol{r}\boldsymbol{i}^H\right] = \frac{1}{2}\mathrm{E}\left[\boldsymbol{r}\boldsymbol{r}^H(\boldsymbol{Z}^{-1})^H\right] \\ &= \frac{1}{2}\boldsymbol{C}\boldsymbol{H}_s\boldsymbol{H}_s^H\boldsymbol{C}^H(\boldsymbol{Z}^{-1})^H \\ &= \boldsymbol{U}\mathrm{diag}\left[\lambda'_1, ..., \lambda'_{m_0}\right]\boldsymbol{V}, \end{aligned} \tag{10}$$

$$\boldsymbol{Z} = \mathrm{diag}\,[Z_{L1}, Z_{L2}, \ldots, Z_{Lm0}], \tag{11}$$

where $\boldsymbol{r}$ is a receiving voltage vector whose elements are the voltages across the terminated loads, and $\boldsymbol{i}$ is the corresponding receiving current vector. The $E[\cdot]$ denotes the ensemble average; λ'_i represents the i-th complex eigenvalue of $\boldsymbol{R}_p$, which corresponds to the received power of the i-th eigen-path. The effective power is thus $\mathrm{Re}[\lambda'_i]$. A water-filling scheme is used to distribute the transmitted signal power on the basis of the effective eigen-path power. The power distribution coefficient corresponding to the j-th eigen-path is determined by

$$p_j = \max\left(\mu - \frac{1}{\gamma_0 \mathrm{Re}\left[\lambda'_j\right]}, 0\right), \tag{12}$$

NII-Electronic Library Service

Institute of Electronics, Information, and Communication Engineers

$$\gamma_0 = \frac{P_x}{2\sigma^2}, \tag{13}$$

where P_x and σ^2 are the total transmitted power and the noise power, respectively. Coefficient μ is defined to satisfy $\sum_{j=1}^{m0} p_j = 1$. Therefore, the capacity of a MIMO system using the water-filling scheme is

$$C_{MIMO} = \sum_{j=1}^{m_0} \log_2 \left(1 + \frac{p_j \mathrm{Re}\left[\lambda'_j\right]}{\sigma^2} \right). \tag{14}$$

2.4 Antenna Matching

As described by Wallace and Jensen [3], the received power and characteristics of the path correlation can be improved by inserting an appropriate matching network. The mutual coupling plays an important role, especially when the element spacing is close. The multiport optimization scheme [3], [4] produces an optimal solution that maximizes the MIMO channel capacity. However, it is sometimes difficult to implement in an actual system. Achieving an appropriate antenna matching that maximizes the received power is relatively easy. It produces a sub-optimal solution for a MIMO receiver. However, the appropriate antenna matching (impedance matching) condition for the MIMO system is not still clear.

Here we focus on the impedance matching condition at the receiving array. More specifically, we model the receiver using only its internal impedance, i.e., the load impedance at each port (Z_{L1}, Z_{L2}), as shown in Fig. 2. Three types of the antenna matching schemes are considered here.

- Z_{11}^* match ($Z_{L1} = Z_{L2} = Z_{11}^*$): conjugate matching to an antenna element, where each port is terminated by the complex conjugate of the element impedance, Z_{ii}. Z_{ii} is the impedance of the i-th element without consideration of the other elements.
- Z_{in}^* match ($Z_{L1} = Z_{L2} = Z_{in}^*$): conjugate matching to the port impedance, where each port is terminated by the conjugate of the port input impedance, Z_{in}^*.
- optimal antenna match: optimal antenna matching to maximize MIMO channel capacity at the receiver. The terminated loads are estimated numerically by changing the resistances and reactances every 1 Ω.

The * above denotes the complex conjugate operator. Note that the load impedance with Z_{11}^* match is unchanged in the element spacings while the load impedance with Z_{in}^* and optimal antenna matching is variable in the spacings. The Z_{in}^* matching is the conventional matching scheme used by antenna engineers. These comparisons illustrate the role of antenna matching in the MIMO receiver.

The self and mutual impedances of a two-element dipole array calculated by Wallace and Jensen [3] (Fig. 4) seem to be slightly biased in narrow spacings. They can also be calculated using Gupta's method [5], but this method cannot accurately calculate the mutual coupling of a receiving array with closely spaced elements [6], [7]. We thus use exact mutual coupling matrices in the receiving array by using external reference waves (see Appendix for details [6]).

3. Simulation

3.1 Simulation Setup

To generate Rayleigh fading, we assumed Jakes model with many scattering points surrounding the receiving array, as shown in Fig. 3. The channel matrix, $\boldsymbol{H}_s$, is derived numerically from Jakes model. There are 20 scattered points randomly located on the circle. We set the distance from the receiving array to each scattered point long enough in comparison with the wavelength so as to realize plane wave incidence on the receiving array. The carrier frequency of the wave is 2.4 GHz. The receiving array has two elements. The configuration of the array is shown in Fig. 4. Two kinds of dipole arrays are evaluated here. The parameters of the elements in each array are listed in Table 1. The elements in Array A have the same parameters as those used by Wal-

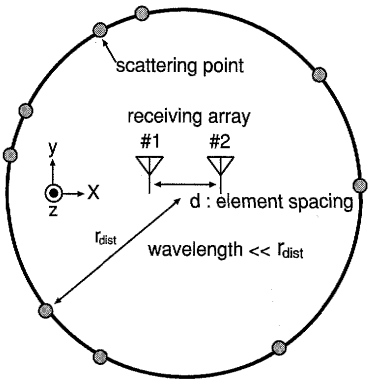

Fig. 3 Scattering channel model.

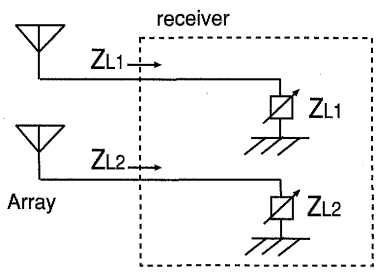

Fig. 2 Model of array and receiver.

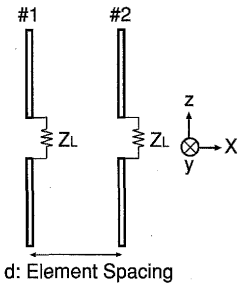

Fig. 4 Array configuration.

NII-Electronic Library Service

Institute of Electronics, Information, and Communication Engineers

Table 1 Element parameters of dipole array.

	Array A	Array B
Element length	6.26 [cm]	5.78 [cm]
Element radius	0.125 [cm]	0.05 [cm]
Self impedance	$105 + j49\,[\Omega]$	$72 + j0\,[\Omega]$

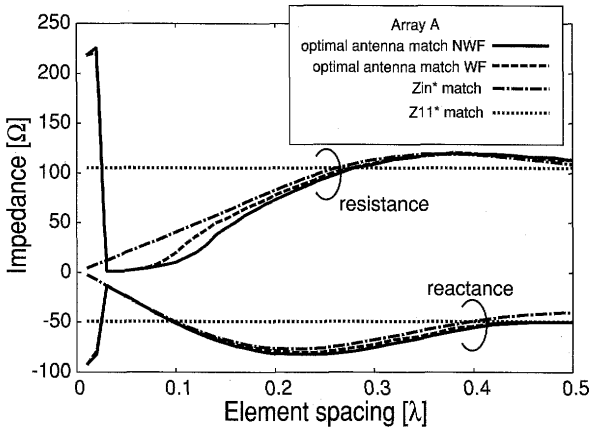

Fig. 5 Load impedance (Array A).

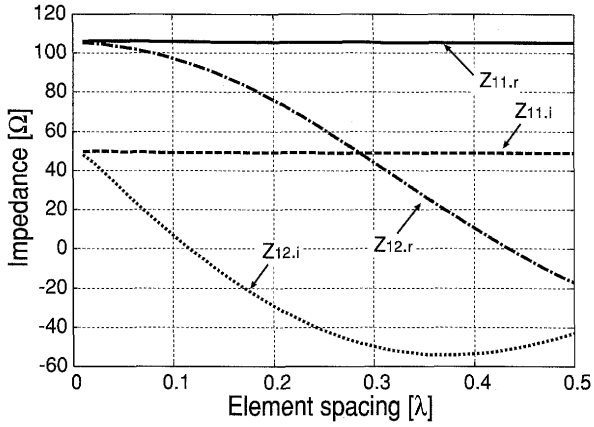

Fig. 6 Self and mutual impedances of array (Array A).

lace and Jensen [3]. The self-impedance of each element is almost $105 + j49\,\Omega$ at 2.4 GHz; therefore, the elements are not well matched at the frequency. On the other hand, the elements in Array B are almost perfectly matched at the frequency. Note that the relation $Z_{L1} = Z_{L2}$ holds for any matching scheme and any kind of element due to the use of a two-element uniform array. Two kinds of power distribution schemes, water-filling (WF) and uniform distribution (NWF), were considered in each simulation.

3.2 Simulation Results

The simulated load impedances for the optimal antenna match, Z_{in}^* match, and Z_{11}^* match using array A are plotted in Fig. 5 as a function of element spacing. Note that the impedances for the optimal antenna match are shown for both the WF and NWF schemes. The self and mutual impedances of the array A at each spacing are depicted in Fig. 6. We will discuss this impedance variation in Sect. 4.

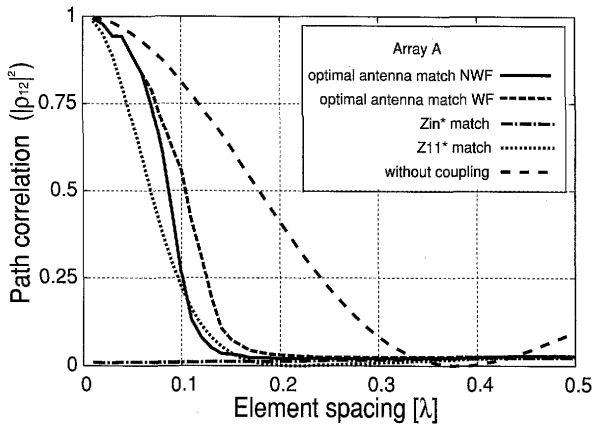

Fig. 7 Path correlation (Array A).

The path correlation, which affects the eigen-path distribution of the MIMO channel, is used as a metric for assessing diversity performance. It is defined by

$$\rho_{ij} = \frac{\sum_{k=1}^{M} \mathrm{E}[h_{ik}^* h_{jk}]}{\sqrt{\sum_{k=1}^{M} \mathrm{E}[h_{ik} h_{ik}^*]}\sqrt{\sum_{k=1}^{M} \mathrm{E}[h_{jk} h_{jk}^*]}}. \tag{15}$$

The magnitudes of the path correlation versus the element spacing are plotted in Fig. 7. These curves show that the path correlation significantly depends on the antenna load, or antenna matching. Interestingly, the Z_{in}^* match effectively destroys the path correlation for almost all the element spacings. In the other matching solutions, the path correlation increases as the element spacing (d) decreases for $d \leq 0.15\lambda$ and reaches one when $d \to 0$. Comparison of these results to those without mutual coupling shows that the correlation was improved by the coupling for all of the matching loads. This is because the element pattern changes due to the coupling. This effect is illustrated in Fig. 8, which plots the pattern of antenna element #1 in the horizontal plane at a spacing of 0.05λ. The pattern of element #2, located in the 0° direction, is symmetrical to that of #1. This means that element #1 receives waves coming mainly from the 0° direction, while element #2 receives them mainly from the 180° direction in the Z_{in}^* matching. Since this is a Rayleigh fading environment, the signal correlation between the two directions is zero. This is why the Z_{in}^* matching has low path correlation for close element spacing.

Furthermore, this element pattern also explains the physical reason for the load impedance with the optimal antenna matching changing rapidly when the element spacing is close. As shown in Fig. 8, we can obtain a high gain element pattern as an endfire array in this matching. This pattern can be understood as that of a super-gain antenna. The load impedance for the optimal antenna matching in Fig. 5 is the impedance that results in the current distribution on the array elements for a super-gain antenna.

The received power is an important factor in the channel capacity as well as in the path correlation. The received powers in the NWF and WF schemes are depicted in Figs. 9 and 10, respectively. They are normalized by the results

NII-Electronic Library Service

Institute of Electronics, Information, and Communication Engineers

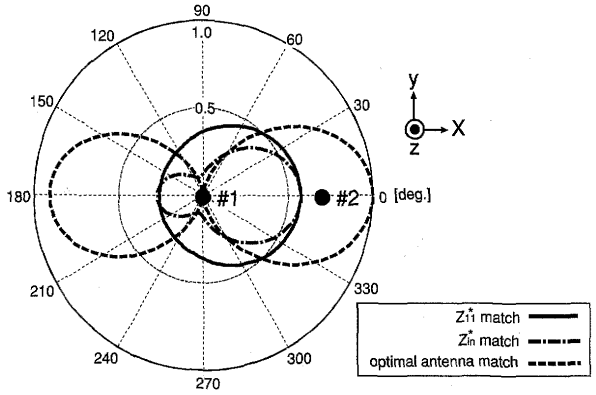

Fig. 8 Received power patterns of element #1 in optimal antenna match, Z_{in}^{*} match and Z_{11}^{*} match for vertical polarized incoming plane wave.

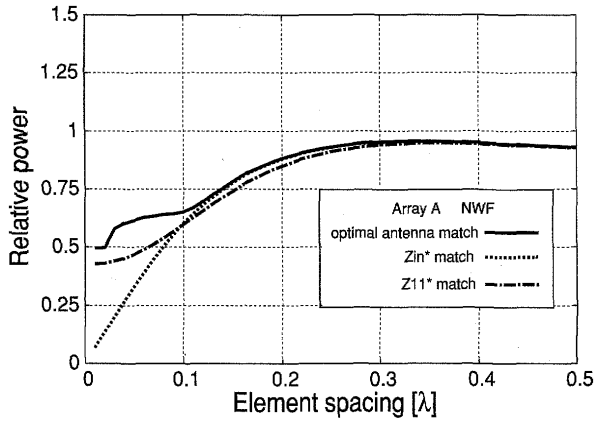

Fig. 9 Received power (NWF, Array A).

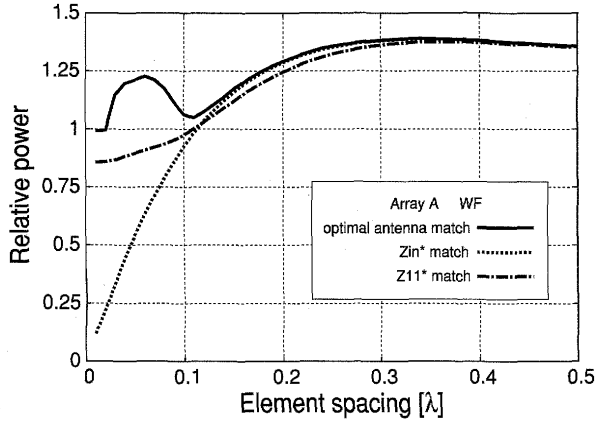

Fig. 10 Received power (WF, Array A).

for an ideal receiving array with the NWF scheme (element spacing is infinite) enabled so that the mutual coupling and spatial correlation are ignored. Though the Z_{in}^{*} match shows low correlation characteristics in Fig. 7, the received power drops significantly as the element spacing approaches zero. Interestingly, for the optimal antenna match, this reduction tendency is weaker in the region where $d \leq 0.1\lambda$. A comparison of the results for the NWF and the WF schemes shows that high received power can generally be obtained by using the WF scheme.

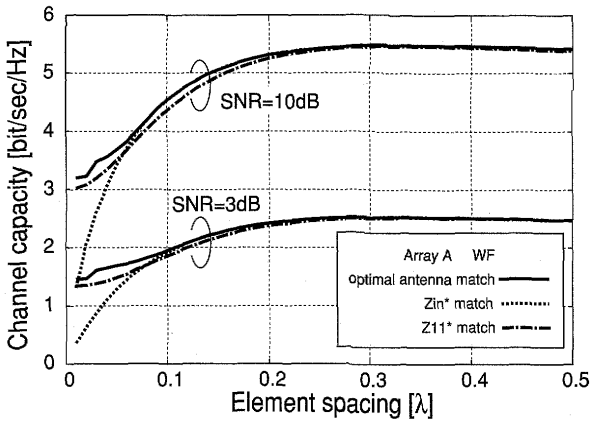

Fig. 11 Channel capacity (SNR 3 dB and 10 dB, NWF, Array A).

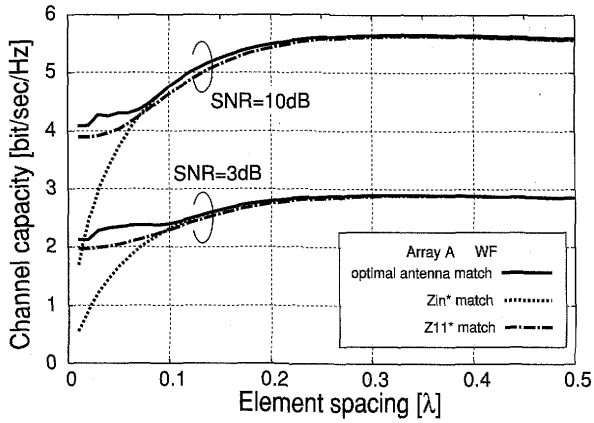

Fig. 12 Channel capacity (SNR 3 dB and 10 dB, WF, Array A).

The channel capacity without and with water-filling for SNR = 3 and 10 dB is shown in Figs. 11 and 12, respectively. The SNR is defined by the average received signal power-to-noise ratio for SISO with Z_{11}^{*} matching. These results show that the performance deterioration due to the spatial correlation of the MIMO receiver is quite small, even when the element spacing is wider than 0.2λ. In addition, the Z_{in}^{*} antenna matching can be used as the optimal antenna matching when the element spacing is wider than approximately 0.1λ.

Since the spatial correlation is quite high for close antenna spacings, $d < 0.1\lambda$, the maximum capacity is effectively obtained by selecting the load impedance that maximizes the received power as much as possible rather than the one that maximizes the number of effective eigen-paths by reducing the path correlation. This corresponds to the MRC (Maximum Ratio Combining) operation in the MIMO receiving array. The Z_{in}^{*} match is the matching solution that reduces the correlation even if the received power decreases. Figure 13 shows the eigen-path powers for the optimal antenna match and for the Z_{in}^{*} match. It illustrates the decorrelation with the Z_{in}^{*} match and the MRC operation with the optimal antenna match. These features are essentially the same at other SNRs (10 dB in these examples).

These results are supported by the simulation results for another array, array B, having the parameters shown in

NII-Electronic Library Service

Institute of Electronics, Information, and Communication Engineers

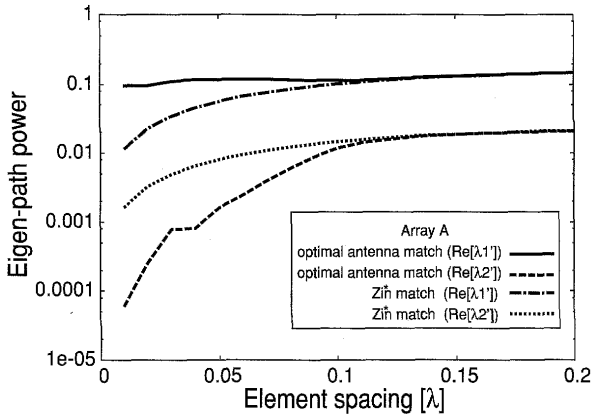

Fig. 13 Eigen-path power (Array A).

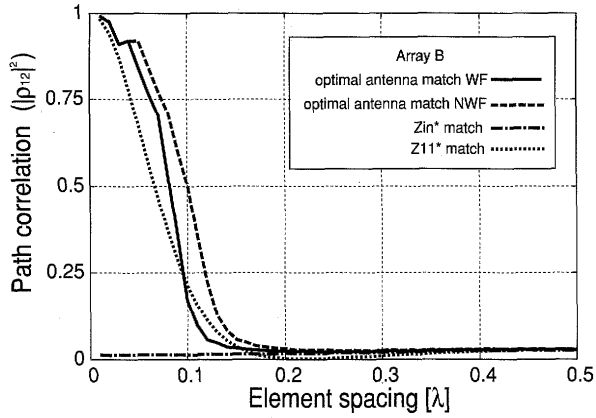

Fig. 14 Path correlation (Array B).

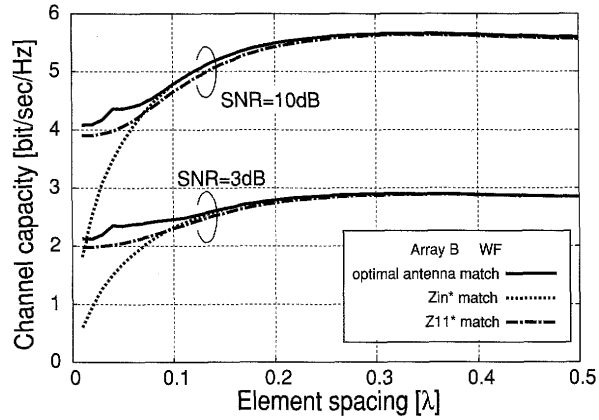

Fig. 15 Channel capacity (SNR 3 dB and 10 dB, WF, Array B).

Table 1. Figures 14 and 15 show the results corresponding to those shown in Figs. 7 and 12, respectively. While this array has different impedance characteristics from those of array A at the given operating frequency, the path correlation and channel capacity have almost the same tendencies. This means that the results of these simulations are applicable to dipole arrays.

4. Theoretical Consideration of Received Power

The capacity of a MIMO receiver with a closely spaced element array strongly depends not only on the path correlation but also on the received power because of the high path correlation. Theoretical consideration of the received power and channel capacity as a function of load impedance is difficult as discussed in [3]. However, for an extreme case ($d \to 0$), we can derive the received power theoretically. Here we provide theoretical results for the received power of two-element arrays. They help clarify and and verify the simulation results presented above. For simplicity, we consider the power for only the NWF transmission scheme. The relation between the terminal voltage vector ($\boldsymbol{v}$) of an array with coupling and the open-circuit voltage ($\boldsymbol{v}_{\text{open}}$) of an array without coupling can be modeled by [5]

$$\boldsymbol{v}_{\text{open}} = \begin{bmatrix} 1+\frac{Z_{11}}{Z_L} & \frac{Z_{12}}{Z_L} \\ \frac{Z_{12}}{Z_L} & 1+\frac{Z_{11}}{Z_L} \end{bmatrix} \boldsymbol{v} = \tilde{\boldsymbol{Z}}\boldsymbol{v} = \boldsymbol{C}^{-1}\boldsymbol{v}, \tag{16}$$

where $Z_{11} = Z_{22}$ and $Z_{12} = Z_{21}$ hold for the two-element array. Mutual coupling matrix $\boldsymbol{C}$ is expressed by

$$\boldsymbol{C} = \frac{Z_L}{(Z_{11}+Z_L)^2 - Z_{12}^2} \begin{bmatrix} Z_{11}+Z_L & -Z_{12} \\ -Z_{12} & Z_{11}+Z_L \end{bmatrix}. \tag{17}$$

4.1 Received Power in Z_{11}^* Matching

Since the load impedance is $Z_L = Z_{11}^* (= R_{11} - jX_{11})$ in this matching, mutual coupling matrix $\boldsymbol{C}$ is

$$\boldsymbol{C} = \frac{R_{11} - jX_{11}}{(2R_{11})^2 - Z_{12}^2} \begin{bmatrix} 2R_{11} & -Z_{12} \\ -Z_{12} & 2R_{11} \end{bmatrix}. \tag{18}$$

When d approaches zero, (18) can be rewritten as follows by using the relation $Z_{11} = Z_{12}$ from in Fig. 6

$$\boldsymbol{C} = \frac{R_{11} - jX_{11}}{3R_{11}^2 - 2jR_{11}X_{11} + X_{11}^2} \begin{bmatrix} 2R_{11} & -(R_{11}+jX_{11}) \\ -(R_{11}+jX_{11}) & 2R_{11} \end{bmatrix}. \tag{19}$$

In addition, the voltage induced by the plane wave at each element are the same, $\boldsymbol{v}_{open} = [v_0, v_0]^T$, because $d \to 0$. Therefore, we can obtain the terminal voltages by using

$$v_1 = v_2 = \frac{(Z_{11}^*)^2}{4R_{11}^2 - Z_{11}^2} v_0. \tag{20}$$

Using this equation, we can represent the power at each element in Z_{11}^* matching by

$$P_{Z_{11}^*} = \frac{1}{2}\text{Re}[v_1 i_1^*] = \frac{1}{2} \frac{R_{11}(R_{11}^2+X_{11}^2)|v_0|^2}{(3R_{11}^2+X_{11}^2)^2 + 4R_{11}X_{11}^2}. \tag{21}$$

For the case of an isolated one-dipole receiver, the received power and terminal voltage are

$$v = \frac{Z_L}{Z_{11}+Z_L} v_0 = \frac{R_{11} - jX_{11}}{2R_{11}} v_0, \tag{22}$$

$$P_0 = \frac{1}{2}\text{Re}[vi^*] = \frac{|v_0|^2}{8R_{11}}. \tag{23}$$

The power normalized by the received power of an isolated

NII-Electronic Library Service

Institute of Electronics, Information, and Communication Engineers

dipole is

$$\frac{P_{Z_{11}^*}}{P_0} = \frac{4R_{11}^2(R_{11}^2 + X_{11}^2)}{(3R_{11}^2 + X_{11}^2)^2 + 4R_{11}^2X_{11}^2}. \quad (24)$$

$$\left(\text{e.g. } R_{11} = 105,\ X_{11} = 50,\quad \frac{P_{Z_{11}^*}}{P_0} = 0.433\right)$$

This agrees with the simulation result for Z_{11}^* match shown in Fig. 9.

4.2 Received Power in Z_{in}^* Matching

Since the load impedance is defined by $Z_L = Z_{in}^*$ in this matching, when we feed $V_g = 1$ to element #1 in the array, the relation between port current $\boldsymbol{i}$ and port voltage $\boldsymbol{v}'$ is given by

$$v_1' = 1 - Z_L i_1 = Z_{11}i_1 + Z_{12}i_2, \quad (25)$$

$$v_2' = -Z_L i_2 = Z_{12}i_1 + Z_{11}i_2. \quad (26)$$

From (25), we can obtain $Z_{in}^* = Z_{11} + Z_{12}i_2/i_1$. The unknown current term, i_2/i_1, can be eliminated by using (26):

$$Z_L = Z_{in}^* = Z_{11}^* + Z_{12}^*\left(-\frac{Z_{12}}{Z_{11} + Z_L}\right)^*. \quad (27)$$

As shown in Fig. 6, Z_{12} approaches to Z_{11} when d tends to zero. In such a case, we can derive the following equation by (27)

$$|Z_L|^2 = -j2R_{11}X_L - 2X_{11}X_L. \quad (28)$$

Clearly, $|Z_L|^2$ is a real valued term, hence $2R_{11}X_L$ must be zero. To satisfy this equation, $X_L = 0$ is required because $R_{11} \neq 0$. Therefore we can derive $Z_L = 0$. Since the load impedance becomes zero, the received power becomes zero as shown in Fig. 9.

4.3 Received Power in Optimal Antenna Matching

The optimal antenna matching loads for $d \to 0$ correspond to the loads that maximize the received power. The received power at each element for $d \to 0$ is by

$$P = \frac{1}{2}\frac{R_L|v_0|^2}{(R_L + 2R_{11})^2 + (X_L + 2X_{11})^2}, \quad (29)$$

where v_0 is the voltage induced by the incident waves as used in the derivation of (20). The maximum received power can be determined by differentiating the equation with respect to R_L and X_L. The maximum power can be obtained at $Z_L = 2Z_{11}^*$, and this becomes $P_{2Z_{11}^*} = |v_0|^2/(16R_{11})$. The power normalized by the received power of an isolated dipole is

$$\frac{P_{2Z_{11}^*}}{P_0} = \frac{8R_{11}|v_0|^2}{16R_{11}|v_0|^2} = 0.5\,. \quad (30)$$

This corresponds to the optimal antenna match (NWF) for $d \to 0$ as shown in Fig. 9.

5. Conclusions

We have analyzed the effect of the mutual coupling of a two-element dipole array receiver in a MIMO system. Three types of impedance matching were considered: Z_{11}^* matching, Z_{in}^* matching, and optimal antenna matching. The effects of mutual coupling with these matchings were examined using computer simulation. In addition, for the special case in which the element spacing tends to zero, theoretical calculations were also done.

The simulation results indicate that conjugate matching, Z_{in}^* match, is the optimal antenna matching for MIMO dipole arrays when the element spacing is wider than 0.1 λ. In addition, the channel capacity becomes almost constant when the element spacing is wider than 0.2 λ. These results will be helpful to antenna designers.

The simulation results also show that the channel capacity can be recovered to some extent by selecting optimal antenna loads; however, these are the point frequency discussion. As shown in Fig. 6, the optimal antenna matched loads drastically changes to the element spacings in narrow spacing region. A MIMO receiver with such close spacing between elements would be a narrow band receiver, so an analysis of the capacity in the operating bandwidth is needed. Also, the optimal matching loads and Z_{in}^*, that were used were numerically derived. An analytical solution is needed to simplify the system design. This will be done in near future.

Acknowledgments

This work was supported by a Grant-in-Aid for Development of Scientific Research from the Japan Society for the Promotion of Science.

References

[1] D. Gesbert, M. Shafi, D.S. Shiu, P. Smith, and A. Naguib, "From theory to practice: An overview of MIMO space-time coded wireless systems," IEEE J. Sel. Areas Commun., vol.21, no.2, pp.281–302, April 2003.

[2] V. Jungnickel, V. Pohl, and C.V. Helmolt, "Capacity of MIMO systems with closely spaced antennas," IEEE Commun. Lett., vol.7, no.8, pp.361–363, Aug. 2003.

[3] J.W. Wallace and M.A. Jensen, "Mutual coupling in MIMO wireless systems: A rigorous network theory analysis," IEEE Trans. Wireless Commun., vol.3, no.4, pp.1317–1325, July 2004.

[4] J.B. Anderson and H.H. Ramussen, "Decoupling and descattering networks for antennas," IEEE Trans. Antennas. Propag., vol.AP-24, pp.841–846, Nov. 1976.

[5] I.J. Gupta and A.A. Ksienski, "Effect of mutual coupling on the performance of adaptive arrays," IEEE Trans. Antennas Propag., vol.AP-31, no.5, pp.785–791, Sept. 1983.

[6] H. Yamada, Y. Ogawa, and Y. Yamaguchi, "On mutual impedance of a receiving array antenna and its calibration matrix," IEICE Technical Report, A·P2004-332, March 2005.

[7] R.S. Adve and T.K. Sarkar, "Compensation for the effects of mutual coupling on direct data domain adaptive algorithms," IEEE Trans. Antennas Propag., vol.48, no.1, pp.86–94, Jan. 2000.

NII-Electronic Library Service

Institute of Electronics, Information, and Communication Engineers

[8] Numerical Electromagnetic Code NEC2 unofficial home page, http://www.nec2.org/

Appendix: Estimation of Mutual Coupling Matrix C

A dipole array has a DOA (direction-of-arrival) independent mutual coupling matrix $\boldsymbol{C}$, so the matrix can be easily derived when we can use external reference incidences of known DOAs. We denote the voltage vector of the loaded array as $\boldsymbol{v}^{(i)}$, which includes the coupling effects, and the coupling-free open terminal voltage vector as $\boldsymbol{v}_0^{(i)}$. The coupling-free open terminal voltage of the j-th element is the voltage induced by the incident wave(s) without considering the other elements. It can be easily derived numerically. In this study, antenna arrays were analyzed using the method of moments (NEC2) [8]. The vectors, $\boldsymbol{v}$ and $\boldsymbol{v}_0$, are related by the coupling matrix:

$$\boldsymbol{v}^{(i)} = \boldsymbol{C}\boldsymbol{v}_0^{(i)}. \tag{A·1}$$

When there are M independent known DOA data sets, we obtain the following equations.

$$[\boldsymbol{v}^{(1)}, \boldsymbol{v}^{(2)}, \ldots, \boldsymbol{v}^{(M)}] = \boldsymbol{C}[\boldsymbol{v}_0^{(1)}, \boldsymbol{v}_0^{(2)}, \ldots, \boldsymbol{v}_0^{(M)}],$$
$$\tilde{\boldsymbol{R}} = \boldsymbol{C}\tilde{\boldsymbol{R}}_0. \tag{A·2}$$

Therefore, the exact mutual coupling matrix in the receive array can be expressed as

$$\boldsymbol{C} = \tilde{\boldsymbol{R}}(\tilde{\boldsymbol{R}}_0)^H(\tilde{\boldsymbol{R}}_0\tilde{\boldsymbol{R}}_0^H)^{-1}. \tag{A·3}$$

Hiroki Iura received a B.E. and M.E. degrees in information engineering from Niigata University, Niigata, Japan, in 2004 and 2006, respectively. He joined Mitsubishi Electric Corporation, Tokyo, Japan, in 2006, and has been engaged in the research and development on mobile communications and MIMO systems. He is currently with the Wireless IP Access Technology Department of Information Technology R&D Center there.

Hiroyoshi Yamada received the B.E., M.E. and Dr.Eng. degrees in electronic engineering from Hokkaido University, Sapporo, Japan, in 1988, 1990 and 1993, respectively. In 1993, he joined the Faculty of Engineering, Niigata University, where he is an associate professor. From 2000 to 2001, he was a Visiting Scientist at the Jet Propulsion Laboratory, California Institute of Technology, Pasadena. His current interests include superresolution techniques, array signal processing, and microwave remote sensing and imaging. Dr. Yamada is a member of the IEEE.

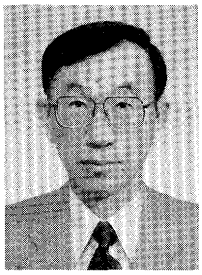

Yasutaka Ogawa received B.E., M.E. and Ph.D. degrees from Hokkaido University, Sapporo, Japan, in 1973, 1975 and 1978, respectively. Since 1979, he has been with Hokkaido University, where he is currently a Professor of the Graduate School of Information Science and Technology. During 1992 and 1993, he was a visiting scholar in the Electro Science Laboratory of Ohio State University. His interests include adaptive antennas, MIMO systems, mobile communications, and superresolution techniques. Dr. Ogawa is a senior member of the IEEE.

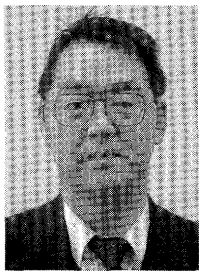

Yoshio Yamaguchi received a B.E. degree in electronics engineering from Niigata University in 1976 and M.E. and Dr.Eng. degrees from the Tokyo Institute of Technology in 1978 and 1983, respectively. In 1978, he joined the Faculty of Engineering, Niigata University, where he is a professor. During 1988 and 1989, he was a research associate at the University of Illinois, Chicago. His interests include the propagation characteristics of electromagnetic waves in a lossy medium, radar polarimetry, and microwave remote sensing and imaging. Dr. Yamaguchi is a fellow of the IEEE.

NII-Electronic Library Service